Dissemination and Systemic Colonization of Uropathogenic *Escherichia coli* in a Murine Model of Bacteremia

Sara N. Smith,[a] Erin C. Hagan,[a] M. Chelsea Lane,[b] and Harry L. T. Mobley[a]

Department of Microbiology and Immunology, University of Michigan Medical School, Ann Arbor, Michigan, USA,[a] and Department of Microbiology and Immunology, University of North Carolina School of Medicine, Chapel Hill, North Carolina, USA[b]

ABSTRACT **Infection with uropathogenic *Escherichia coli* (UPEC), the causative agent of most uncomplicated urinary tract infections, proceeds in an ascending manner and, if left untreated, may result in bacteremia and urosepsis. To examine the fate of UPEC after its entry into the bloodstream, we developed a murine model of sublethal bacteremia. CBA/J mice were inoculated intravenously with 1×10^6 CFU of pyelonephritis strain *E. coli* CFT073 carrying a bioluminescent reporter. Biophotonic imaging, used to monitor the infection over 48 h, demonstrated that the bacteria disseminated systemically and appeared to localize at discrete sites. UPEC was recovered from the spleen, liver, kidneys, lungs, heart, brain, and intestines as early as 20 min postinoculation, peaking at 24 h postinoculation. A nonpathogenic *E. coli* K-12 strain, however, disseminated at significantly lower levels ($P < 0.01$) and was cleared from the liver and cecum by 24 h postinoculation. Isogenic mutants lacking type 1 fimbriae, P fimbriae, capsule, TonB, the heme receptors Hma and ChuA, or particularly the sialic acid catabolism enzyme NanA were significantly outcompeted by wild-type CFT073 during bacteremia ($P < 0.05$), while flagellin and hemolysin mutants were not.**

IMPORTANCE ***E. coli* is the primary cause of urinary tract infections. In severe cases of kidney infection, bacteria can enter the bloodstream and cause systemic disease. While the ability of *E. coli* to cause urinary tract infection has been extensively studied, the fate of these bacteria once they enter the bloodstream is largely unknown. Here we used an imaging technique to develop a mouse model of *E. coli* bloodstream infection and identify bacterial genes that are important for the bacteria to spread to and infect various organs. Understanding how urinary tract pathogens like *E. coli* cause disease after they enter the bloodstream may aid in the development of protective and therapeutic treatments.**

Received 7 October 2010 **Accepted** 27 October 2010 **Published** 23 November 2010

Citation Smith, S. N., E. C. Hagan, M. C. Lane, and H. L. T. Mobley. 2010. Dissemination and systemic colonization of uropathogenic *Escherichia coli* in a murine model of bacteremia. mBio 1(5):e00262-10. doi:10.1128/mBio.00262-10.

Editor Rino Rappuoli, Novartis Vaccines and Diagnostics

Address correspondence to Harry L. T. Mobley, hmobley@umich.edu.

Uropathogenic *Escherichia coli* (UPEC), a subset of extraintestinal pathogenic *E. coli* (ExPEC), is the causative agent of most cases of uncomplicated urinary tract infection (UTI). UTIs proceed in an ascending manner, beginning with bacterial colonization of the bladder, followed by ascension to the kidneys. In severe cases of pyelonephritis, bacteria can cross the epithelial cells of the proximal tubule and the endothelial cells of the capillary and gain access to the bloodstream, causing bacteremia and occasionally sepsis. In a recent study of bacteremic UTIs, *E. coli* was the most common pathogen, responsible for nearly 75% of all Gram-negative bacteremias (1). Bacteremia, defined as the presence of bacteria in the bloodstream (2), can lead to sepsis, which is a systemic inflammatory response that may lead to organ dysfunction.

Virulence determinants that contribute to UPEC colonization of the urinary tract include fimbrial adhesins (3, 4), flagellin (5), secreted proteins (6), polysaccharide capsule (7), ferric iron acquisition systems (8), and specific metabolic pathways (9, 10). Besides hemolysin, which has been implicated in urosepsis (11), the extent to which these uropathogenicity factors also contribute to virulence once UPEC gains access to the bloodstream is not known. However, extensive epidemiological data have correlated the presence of specific virulence genes, including those for toxins, iron acquisition determinants, and P fimbrial adhesins, with *E. coli* urosepsis (12–14).

Although commensal *E. coli* (2) and UPEC (2, 11) strains have been tested at high doses intravenously, no nonlethal model of pathogenic *E. coli* bacteremia currently exists; ExPEC virulence, however, has been examined using several vertebrate and invertebrate sepsis models. A lethal sepsis mouse model, using a subcutaneous infection route, was able to differentiate pathogenic from nonpathogenic *E. coli* strains (15) and has been used subsequently to assess the virulence of isogenic mutants (16). A similar lethal sepsis model using an intraperitoneal infection route was used to assess the efficacy of putative ExPEC vaccine candidates in mice (17). More recently, nonmammalian models of ExPEC lethality have been explored, including *Caenorhabditis elegans* (18) and African migratory locusts (19). Various ExPEC and nonpathogenic *E. coli* strains were also tested in a lethal zebrafish model of systemic infection which was subsequently used to differentiate the roles of two secreted toxins (21).

While ExPEC sepsis models contribute to the understanding of ExPEC virulence factor function, they may not be reflective of UPEC pathogenesis after entry into the bloodstream. Many sepsis

models involve administration of bacteria through routes other than the bloodstream. Furthermore, bacteria are usually delivered at high doses, leading to massive inflammatory responses and rapid death, therefore representing severe sepsis, not the natural progression of bacteremia. Large bacterial doses also result in the delivery of high concentrations of lipopolysaccharide (LPS), which has profound effects on host inflammation. In contrast, UPEC passage from the kidneys into the bloodstream likely occurs at doses well below the median lethal dose (LD_{50}). While this initial bacteremia can progress to sepsis, it is important to understand the early events that occur after UPEC enters the circulation.

Here, we utilized *in vivo* bioluminescence imaging, used previously to monitor bacterial infections within mammalian hosts (20), to develop a murine model of UPEC bacteremia. This report demonstrates that after intravenous inoculation of a sublethal dose, UPEC disseminates systemically and infiltrates specific tissues; a nonpathogenic *E. coli* K-12 strain is quickly cleared. We also show that several well-characterized urovirulence factors contribute to UPEC dissemination, and we demonstrate the presence of bacteremia-specific fitness factors.

RESULTS

Development of a murine model of bacteremia. To examine the pathogenesis of UPEC in the bloodstream, we developed a murine model of *E. coli* bacteremia. Prototypical pyelonephritis strain *E. coli* CFT073 is a urosepsis strain isolated from both the blood and urine of a patient with acute pyelonephritis (22). Female CBA/J mice were inoculated intravenously via tail vein injection with CFT073 carrying a stable luminescent reporter, pGEN-*lux* (20), at various doses. At 3 h postinoculation (hpi), the bacterial load in the spleen was assessed as an indicator of bacteremia. Bacteria could be recovered from the spleens of animals inoculated with a dose as low as 10^3 CFU/mouse (Fig. 1A). Spleens excised 20 min postinoculation from infected animals were luminescent (Fig. 1C), indicating that the bacteremia was due to CFT073(pGEN-*lux*). The median infectious dose (ID_{50}) was determined to be 10^5 CFU/mouse and yielded a median bacterial load of approximately 10^3 CFU/g spleen. For comparison, the ID_{50} for transurethral inoculation of this urinary isolate is 10^6 CFU/mouse (23). To ensure infection of a larger proportion of the population, 10 times the ID_{50} (10^6 CFU/mouse) was used for all subsequent experiments.

Using biophotonic imaging, infected mice were monitored for signs of bacterial dissemination. Immediately following inoculation (0.3 hpi), the bioluminescent signal was restricted to areas near the injection site in 4 of 10 mice but detected in the upper thoracic region in 6 of 10 mice (Fig. 1B). The spleen isolated from a mouse with ventral luminescence at 0.3 hpi (similar to the mouse shown in Fig. 1B) was also luminescent (Fig. 1C) and contained ~10^5 CFU, indicating that at least part of the whole-animal signal was due to splenic infiltration. Overall, ventrally measured luminescence decreased slightly over time, while the signal detected from the dorsal side increased (Fig. 1D). Indeed, by 24 hpi, an intense luminescent signal was detected in the lower abdomen and sacral area of inoculated mice (Fig. 1B). This signal persisted and appeared to have spread further by the experimental endpoint, 48 hpi. Excision and *ex vivo* imaging of the ileum, cecum, and colon at 48 hpi revealed luminescence in these organs (Fig. 1C), indicating that bacterial colonization in the intestinal tract was at least partially responsible for the abdominal signal observed in live animals. These data suggest that, when introduced into the bloodstream, UPEC is capable of systemic dissemination.

Intravenous inoculation of UPEC leads to tissue infiltration and systemic colonization. To determine the extent to which UPEC disseminates during bacteremia, groups of mice were intravenously challenged with 10^6 CFU CFT073(pGEN-*lux*) and bacteria present in systemic tissues were quantified throughout the infection. Immediately following inoculation (20 min postinoculation), bacteria were present in the spleen, liver, kidneys, lungs, heart, brain, duodenum, ileum, and cecum, with the highest bacterial loads found in the spleen and liver (Fig. 2). Culture plates were imaged, and all colonies were found to be luminescent (Fig. 2F, inset), indicating that the enumerated bacteria represented the inoculated strain.

In most tissues, bacterial colonization decreased over time, although duodenum and cecal colonization remained relatively constant through 48 hpi (Fig. 2G and J). This is consistent with biophotonic imaging data which demonstrate a decrease in upper ventral luminescence and an increase in lower ventral and dorsal signals (Fig. 1). In the liver (Fig. 2B), kidneys (Fig. 2C), lungs (Fig. 2D), heart (Fig. 2E), brain (Fig. 2F), and ileum (Fig. 2I), bacterial loads fell below the limit of detection by 48 hpi. While bacteria present in the liver and kidneys were cleared slowly over the course of the experiment, UPEC bacteria were cleared from the lungs, brain, and ileum as early as 4 hpi and from the heart by 24 hpi. Exceptions were the jejunum (Fig. 2H) and feces (Fig. 2L), where bacteria were not detected until 24 hpi. The colon (Fig. 2K) and bladder (data not shown) were the only organs examined that did not contain bacteria in measurable numbers at any point during infection. Because bioluminescence was observed in the colon *ex vivo* at 48 hpi (Fig. 1C), this suggests that UPEC only sometimes disseminates to the colon or that the luminescent signal detected was due to luminal (or feces-associated) and not tissue-associated bacteria. Taken together, these data indicate that UPEC disseminates systemically during bacteremia and appears to persist in specific intestinal tissues for at least 2 days postinoculation (dpi).

Tissue perfusion does not eliminate bacterial infiltration. One possible explanation for widespread dissemination and organ colonization is that UPEC remains in the bloodstream after inoculation and that the dissemination observed was simply due to bacteria present in organ-associated blood vessels and did not represent colonization of specific tissues. To test this hypothesis, intravenously inoculated mice were perfused immediately after euthanasia at 24 hpi with 40 ml sterile saline before organ excision and processing. Gross organ blanching was used as an indication that blood was depleted from the body and perfusion was complete (24), although complete blanching of the spleen was not observed. Bacterial levels in the liver, cecum, kidneys, and brain were not significantly different between nonperfused and perfused animals (Fig. 3). In contrast, perfusion significantly reduced bacterial levels in the lungs ($P = 0.0196$), with undetectable levels in five of six perfused mice, indicating that nearly all of the bacteria recovered from the lungs were due to circulating UPEC. Perfused mice also had lower levels of bacteria in their spleens ($P = 0.0290$), although the median bacterial load was still greater than 10^4 CFU/g, indicating that both circulating and tissue-associated bacteria contributed to splenic infiltration. Overall, these data show that most of the bacterial infiltration observed was indeed due to tissue colonization and not merely the presence of circulating blood.

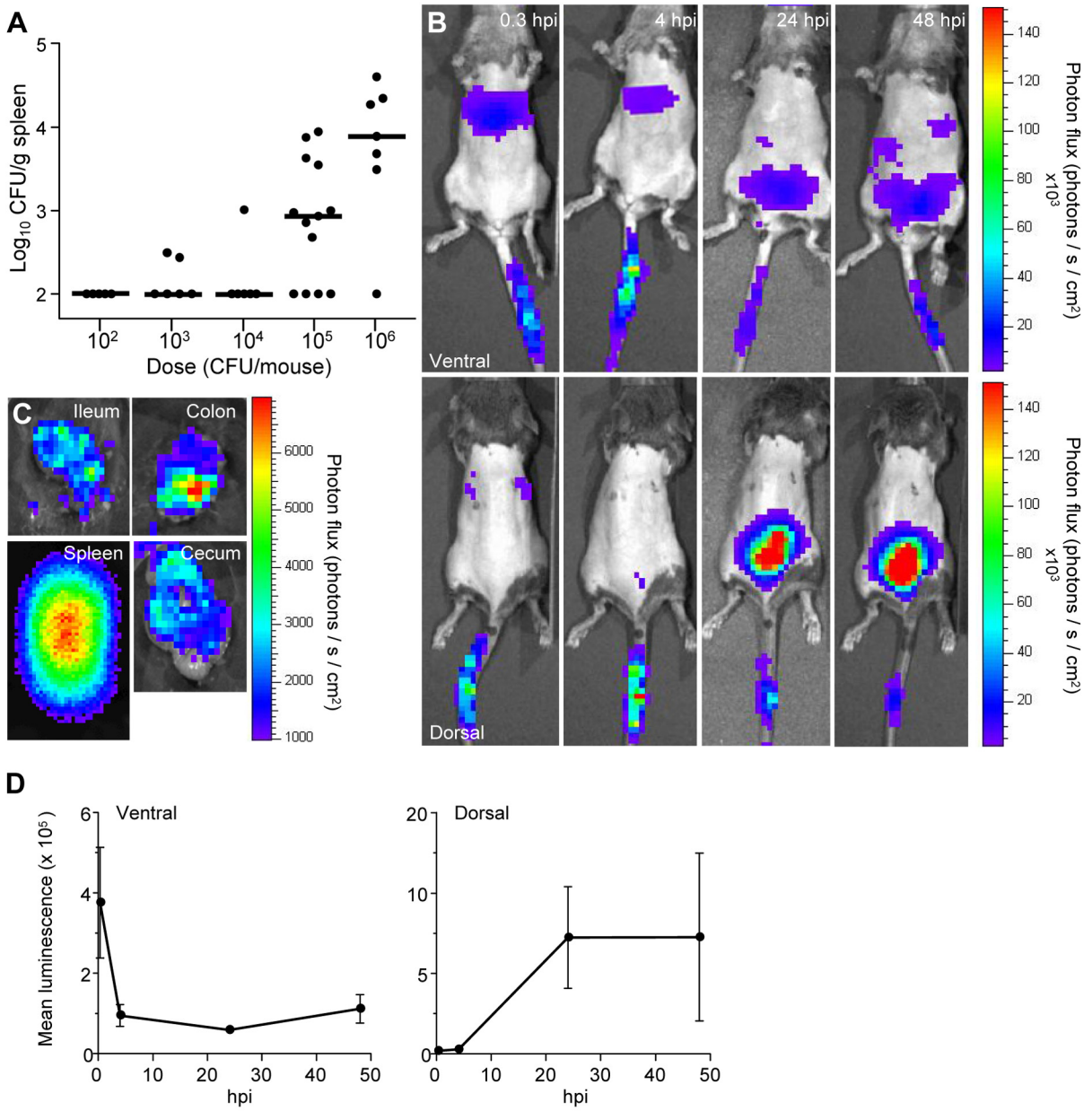

FIG 1 Real-time imaging of UPEC dissemination during bacteremia. (A) Splenic bacterial loads at 3 hpi following intravenous inoculation of CBA/J mice with the indicated doses of *E. coli* CFT073(pGEN-*lux*). Filled circles represent numbers of CFU/g from individual animals, and bars show the medians. The limit of detection was 100 CFU/g. (B) Biophotonic imaging of the ventral (top) and dorsal (bottom) sides of a live mouse at 0.3 (left), 4 (left center), 24 (right center), and 48 (right) h following intravenous inoculation with 10^6 CFU. (C) Biophotonic imaging of an excised spleen (bottom left) at 0.3 h and the ileum (top left), colon (top right), and cecum (bottom right) at 48 h following inoculation as described for panel B. (D) Quantification of luminescence imaged from the thoracic ventral (left) and dorsal (right) sides of mice inoculated as described for panel B. Mean luminescence is shown, and error bars represent the standard error of the mean ($n = 10$).

UPEC systemic colonization persists longer than a commensal *E. coli* strain. To determine whether systemic dissemination by UPEC is a pathogen-specific process or simply represents the natural course of bacterial clearance from the bloodstream, nonpathogenic *E. coli* K-12 strain MG1655 was tested in the bacteremia model. At 24 hpi, the spleen and liver (Fig. 4A) contained significantly lower levels of MG1655(pGEN-*lux*) than CFT073(pGEN-*lux*) ($P = 0.0024$ and $P = 0.0087$, respectively). Mice infected with MG1655 also had lower levels of cecal colonization, although this difference was not significant at 24 hpi. To examine the persistence dynamics of these strains, cecal colonization was examined at up to 7 dpi. Because pGEN-*lux* is only stably maintained in CFT073 for 48 h in the absence of antibiotic selection (20), isogenic *lacZ* mutants of CFT073 and MG1655 were used to allow differentiation from the cecal microbiota. Thus, while it is important to note that this represents a method of bacterial quantification different from that shown previously (Fig. 2 and 4A) that does not depend on the presence of pGEN-*lux*, cecal

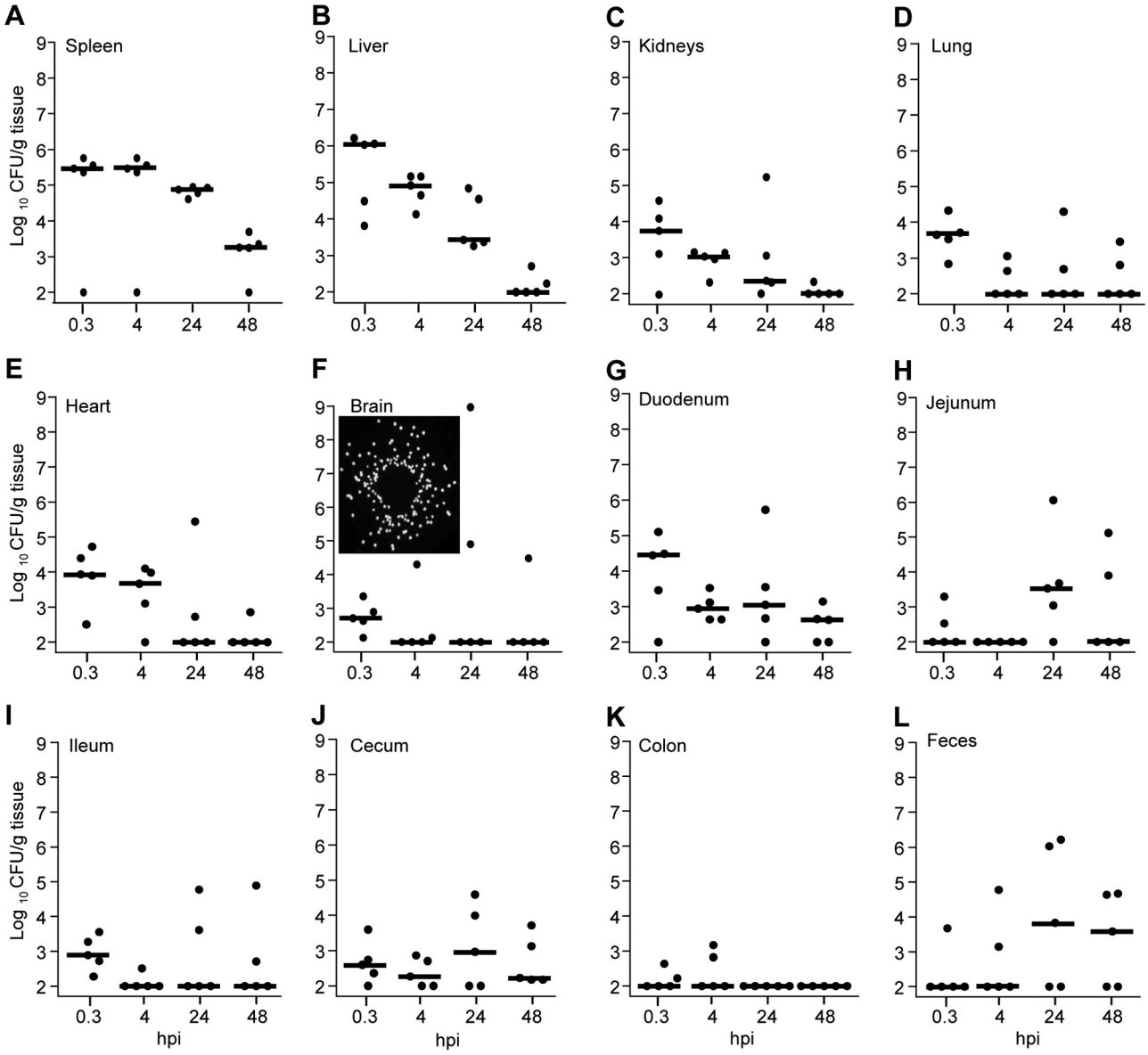

FIG 2 Systemic dissemination of UPEC after intravenous inoculation. Bacterial recovery from the (A) spleen, (B) liver, (C) kidneys, (D) lungs, (E) heart, (F) brain, (G) duodenum, (H) jejunum, (I) ileum, (J) cecum, (K) colon, and (L) feces at 20 min (0.3 h) to 48 hpi intravenously with 10^6 CFU *E. coli* CFT073(pGEN-*lux*). Inset, bioluminescent image of bacterial colonies recovered from brain tissue at 0.3 hpi. Filled circles represent individual mice, and bars show the medians. The limit of detection was 100 CFU/g.

colonization by CFT073(pGEN-*lux*) did not differ from that by CFT073 *lacZ* at 24 hpi (data not shown). While CFT073 colonization persisted in the cecum at 72 hpi at nearly 10^4 CFU/g, *E. coli* MG1655 was cleared by this time point from 9 of 10 mice ($P < 0.0001$) (Fig. 4B). By 7 dpi, CFT073 had been cleared from the ceca of 7 of 10 mice. These data indicate that nonpathogenic *E. coli* is not capable of persisting systemically during bacteremia in this model and suggest that UPEC dissemination and persistence represent pathogenic mechanisms.

Heme acquisition, adherence, capsule, and sialic acid metabolism contribute to UPEC fitness in the bloodstream. The finding that UPEC is more effective at bacteremic dissemination or more resistant to immune clearance than *E. coli* MG1655 is suggests that UPEC-specific factors play a role in systemic colonization. We hypothesized that some, but likely not all, of the genes known to play a role in uropathogenesis may be important for virulence during bacteremia. To address this, isogenic mutants defective for recognized UPEC fitness factors were tested in cochallenge studies in our bacteremia model. Each mutant and the wild type were mixed in equal proportions and inoculated intravenously to yield a total dose of 10^6 CFU per mouse. At 24 hpi, bacteria were quantified in the spleen and liver and competitive indices (CIs) were calculated for each mutant (Table 1).

Both a P fimbria-deficient strain (*pap*) and a type 1 fimbria phase locked-OFF strain that does not produce type 1 fimbriae (*fim* L-OFF) were outcompeted by wild-type CFT073 in the spleen

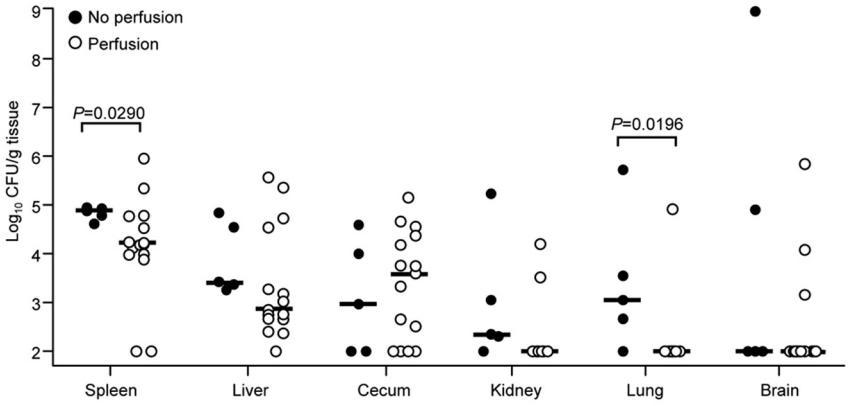

FIG 3 Tissue infiltration following perfusion. Shown are bacterial loads at 24 h following tail vein inoculation of CBA/J mice with 10^6 CFU *E. coli* CFT073(pGEN-*lux*). Organs were harvested immediately (closed symbols) or following postmortem whole-animal cardiac perfusion with 40 ml PBS (open symbols). Data for nonperfused animals (closed symbols) were taken from the experiment shown in Fig. 2. Bars show the medians. The limit of detection was 100 CFU/g. Statistically significant *P* values (<0.05) are indicated.

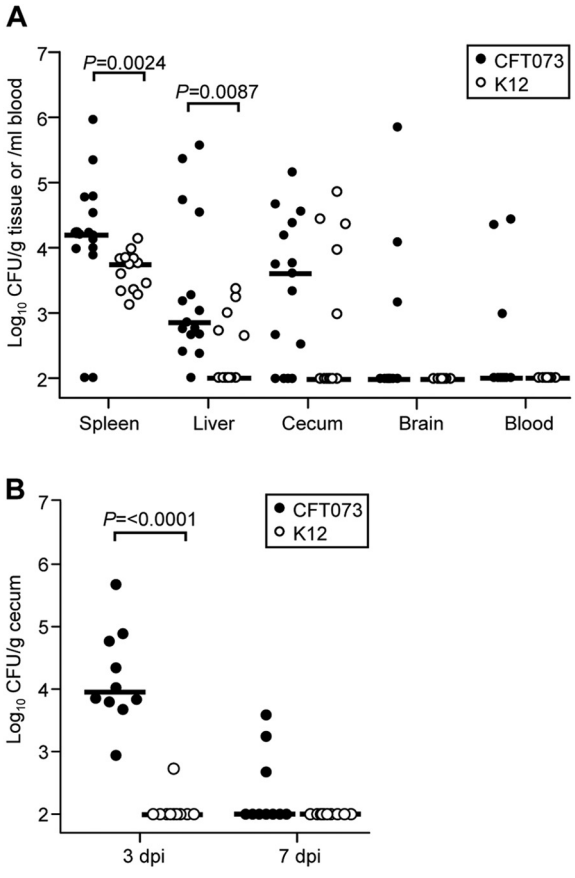

FIG 4 Systemic tissue colonization by and persistence of *E. coli* CFT073 and a commensal K-12 strain. (A) Bacterial loads at 24 h following an intravenous challenge with 10^6 CFU *E. coli* CFT073(pGEN-*lux*) (solid symbols) or *E. coli* K-12 strain MG1655(pGEN-*lux*) (open symbols). (B) Bacterial loads in cecal tissue at 3 and 7 days following an intravenous challenge with 10^6 CFU *E. coli* CFT073 Δ*lacZ* (solid symbols) or *E. coli* K-12 strain MG1655 Δ*lacZ* (open symbols). Symbols represent individual animals, and bars show the medians. The limit of detection was 100 CFU/g. Statistically significant *P* values (<0.05) are indicated.

and liver, indicating that fimbria-mediated adherence contributes to UPEC systemic colonization (Fig. 5). A K2 polysaccharide capsule mutant (*ksl*) found previously to exhibit increased serum susceptibility (7) was outcompeted by $CFT073^{Nal}$ in the spleen and liver also, indicating that capsule contributes to UPEC bacteremic fitness. In contrast, neither a nonmotile flagellin mutant (*fliC*) nor an alpha-hemolysin mutant (*hlyD*), both of which have been shown to contribute to UPEC urovirulence (5, 25), were significantly outcompeted by wild-type CFT073 in either tissue.

Iron acquisition, which is required for UPEC colonization of the urinary tract (8), would be predicted to contribute appreciably to survival in the bloodstream. A *tonB* deletion mutant which is defective for growth under iron limitation was significantly outcompeted in both the spleens and livers of infected mice (Fig. 5), indicating that ferric iron acquisition does contribute to UPEC systemic colonization. To more closely examine the role of iron acquisition during bacteremia, we tested in a cochallenge a heme uptake-defective *hma chuA* mutant which lacks both TonB-dependent heme receptors (26). This mutant was also outcompeted in the spleen and liver during bacteremia, demonstrating that heme uptake contributes to UPEC pathogenesis in this model. Surprisingly, the median CI of the *hma chuA* mutant in the liver was nearly 10-fold lower than that of the *tonB* mutant ($P = 0.0039$), indicating that the *hma chuA* mutant was significantly less fit during bacteremia than the *tonB* mutant was.

UPEC systemic dissemination during bacteremia requires that bacteria utilize carbon sources available in the host. Sialic acid is a major component of erythrocyte membrane glycoproteins, and *E. coli* is able to use this amino sugar as a carbon source (27). Although sialic acid catabolism does not contribute to UPEC fitness in the murine urinary tract (9), we hypothesized that it may contribute to bacterial survival in the bloodstream. The *E. coli* enzyme *N*-acetylneuraminate aldolase, encoded by *nanA*, catalyzes the breakdown of *N*-acetylneuraminic acid, the major sialic acid in mammalian cells, into pyruvate and

TABLE 1 CIs of UPEC virulence factor mutants in a murine cochallenge model of bacteremia

Mutant	Spleen		Liver	
	CI[a]	*P* value	CI	*P* value
fim L-OFF	0.280	0.0039[b]	0.257	0.0391[b]
pap	0.272	0.0039[b]	0.236	0.0039[b]
fliC	0.710	0.1602	0.228	0.0840
hlyD	0.874	0.4922	0.957	0.6953
ksl	0.396	0.0234[b]	0.303	0.0078[b]
tonB	0.353	0.0009[b]	0.264	0.0034[b]
hma chuA	0.183	0.0001[b]	0.043	0.0039[b]
nanA	0.031	0.0078[b]	0.052	0.0078[b]

[a] The median CI for each mutant is shown. It was calculated as follows: $CI = (Mutant_{CFU}/WT_{CFU})_{input}/(Mutant_{CFU}/WT_{CFU})_{output}$.
[b] Statistically significant difference ($P < 0.05$).

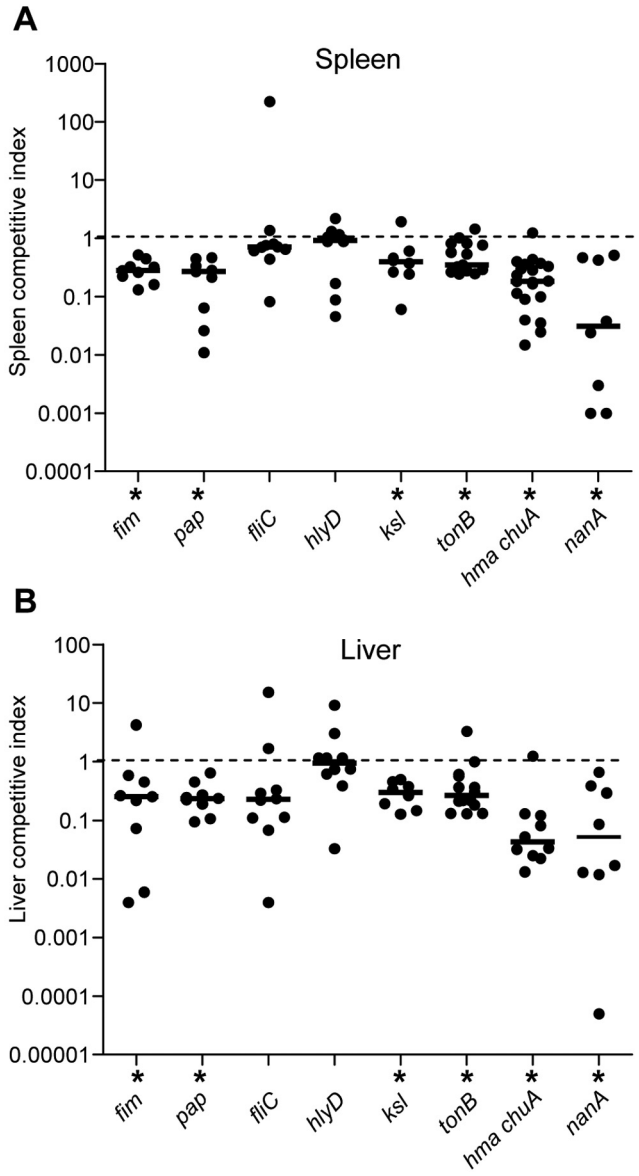

FIG 5 UPEC virulence factor mutants in a cochallenge model of bacteremia. The indicated isogenic mutants were mixed 1:1 with wild-type CFT073 (except for the *ksl* cochallenge, where CFT073^{Nal} was used), and CBA/J mice ($n = 8$ to 20) were inoculated intravenously with 10^6 CFU. CIs are shown for bacterial recovery at 24 hpi in the (A) spleen and (B) liver. Bars indicate the medians, and the dashed line represents a theoretical CI of 1. *, $P < 0.05$.

N-acetylmannosamine. When tested in the bacteremia model, a CFT073 *nanA* mutant was outcompeted by the wild type more than 25-fold in both the spleen and the liver (Fig. 5), indicating that metabolism of *N*-acetylneuraminic acid contributes significantly to systemic dissemination during UPEC bacteremia and suggesting that sialic acids represent important bacterial carbon sources in this niche.

DISCUSSION

This study describes the development and application of a murine model of UPEC bacteremia. Using biophotonic imaging, we demonstrate that UPEC disseminates systemically after intravenous inoculation of a sublethal dose, infiltrating tissues of multiple organs. Colonization is a property of the UPEC strain and is not observed in a laboratory strain. Testing of mutants defective for known urovirulence factors further established that adherence, heme acquisition, capsule, and sialic acid metabolism contribute to UPEC fitness during bacteremic dissemination and systemic colonization independently of their roles in UTI. To our knowledge, this is the first study to examine the fate of a uropathogen once it enters the bloodstream of and disseminates within a mammalian host.

Urosepsis, or sepsis caused by UTI, can occur during severe cases of pyelonephritis when UPEC enters the circulation after crossing the kidney proximal tubule epithelium and capillary endothelial cells. Although vertebrate animal models of systemic ExPEC infection have been utilized to examine *E. coli* sepsis (15), the fate of UPEC upon entry into the mammalian bloodstream at a sublethal dose was unknown. The model described here employs a relatively low inoculation dose and results in both tissue infiltration and colonization. Indeed, no morbidity or mortality was observed in any infected mice, suggesting that neither LPS toxemia nor sepsis was induced. Consequently, use of the ID_{50}, rather than the LD_{50}, to develop a bacteremia model allowed investigation of UPEC infection immediately following bloodstream entry and during subsequent dissemination but before the progression to sepsis.

Over time, systemic bacterial loads generally decreased and 7 of 10 mice were free from detectable colonization by 1 week postinoculation, indicating that in this model, UPEC is cleared from these tissues. In UTI models, infection duration and clearance are influenced significantly by host factors that differ among different inbred mouse strains (28), suggesting that mouse strain-specific factors may also contribute to bacteremia outcome. In this model, clearance is partially dependent on the dose administered, as intravenous inoculation with a 10-fold higher dose of CFT073 (10^7 CFU) resulted in $>10^3$ CFU/g spleen or liver after 1 week (2). This is also in contrast to what has been observed for K1 ExPEC strains, which replicate to high titers in the spleen, blood, and brain following intraperitoneal inoculation of ~10^1 CFU in a neonatal rat model (29). Thus, although this study demonstrates that UPEC with a K2 capsule disseminates and infiltrates tissue during bacteremia, it is clearly not as well adapted to a bacteremic lifestyle as ExPEC strains that produce K1 capsule.

ExPEC strains that produce K1 polysaccharide capsule are associated with neonatal meningitis (30) and have been shown to cross the blood-brain barrier (31). In a neonatal rat model of meningitis, a non-K1 strain was able to invade but not survive in the brain (32). Surprisingly, CFT073, which produces a K2 capsule, was occasionally recovered from the brains of intravenously infected mice and was not eliminated from this site by cardiac perfusion. As cerebrospinal fluid was not quantitatively cultured, it is unclear whether this represents a breach of the blood-brain barrier. It is possible that, instead of penetration of the meninges, the bacterial infiltration observed was due to trace amounts of circulating blood remaining in brain-associated capillaries even after perfusion was completed.

The results shown here suggest that a fraction of the intravenously introduced CFT073 colonizes the gastrointestinal (GI) tract and is excreted by the mouse through this system. As early as 20 min postinoculation, the duodenum had significant levels of bacterial colonization and bacteria persisted in the cecum until at

least 3 dpi. The bacterial load present in feces was densest at later time points (24 and 48 hpi), which is consistent with clearing of the bacteria through the GI tract. The ascending route of a UTI from the fecal site into the urinary tract is considered the primary route of transmission of UPEC. Thus, the finding that UPEC colonizes the GI tract during bacteremia and is subsequently excreted in the feces has implications for UPEC transmission and the potential for reinfection via the ascending route. Similarly, these studies provide evidence against the model of a descending route of UTI, as intravenous UPEC did not establish a persistent infection in the kidneys or bladder.

Introduced intravenously, *pap* and *fim* L-OFF isogenic mutants were outcompeted by the wild type in the spleen and liver, indicating that fimbria-mediated adherence contributes not only to localized infection in the case of the urinary tract but also systemic colonization. Interestingly, although type 1 fimbriae are required by *E. coli* K1 to bind brain endothelial cells (33), a K1 *fim* locked-ON strain that constitutively expresses type 1 fimbriae was unable to induce wild-type bacteremia in a neonatal rat model of meningitis and neither *fim* L-OFF nor Δ*fim* mutants were attenuated for K1 bacteremia (34), suggesting a role for phase variation. Further work is needed to determine whether our results, which demonstrate the contribution of type 1 fimbriae to systemic tissue colonization (but not necessarily bloodstream replication), are consistent with these previous findings or whether they represent a difference between *E. coli* K1 and UPEC bacteremias. P fimbriae, for which a definitive role in UTI has not been established (35), bind to specific digalactoside moieties present on urothelial cells (36) and erythrocytes (37). Together with our findings, this suggests that the ability to adhere to erythrocytes or other host cells may provide UPEC a competitive advantage during bacteremia.

In contrast, flagella and hemolysin, known contributors to UPEC colonization (5) and tissue damage (25) of the murine urinary tract, did not play a significant role in its systemic dissemination or colonization during bacteremia. This is unlike what was observed for UPEC strain 536, which requires pathogenicity islands I and II for lethality in an intravenous murine sepsis model, a phenotype attributed to the loss of two hemolysin determinants (11). Similarly, deletion of an *E. coli* K1 genomic island carrying hemolysin and P fimbrial genes abrogated the ability of this strain to cause neonatal rat bacteremia (38). A systemic role for hemolysin may be strain specific, as Wiles et al. (21) also demonstrated that hemolysin is dispensable for CFT073 systemic infection of zebrafish, although this toxin was required by other UPEC strains.

TonB-dependent ferric iron acquisition systems, which are required for UPEC urinary tract colonization (8), also contribute to UPEC survival during bacteremia. Acquisition of heme, which would be an abundant source of iron in the bloodstream, appears to account for most of the requirement for *tonB*. Surprisingly, the *hma chuA* mutant was significantly less fit in the liver than the *tonB* mutant was. This implies that, in addition to their documented TonB-dependent heme uptake functions (26, 39), Hma and/or ChuA may have TonB-independent functions, such as adherence (40). Alternatively, one or more TonB-dependent receptors may have a negative impact on bacterial survival during UPEC bacteremic dissemination and colonization, perhaps by facilitating antimicrobial uptake, which was alleviated in the *tonB* mutant.

Capsule production is a common virulence factor among ExPEC strains, and K2 capsule is required for CFT073 urinary tract colonization and serum resistance (7). In both UPEC and avian pathogenic *E. coli*, capsule synthesis genes were upregulated during sepsis in chickens (41). K1 polysialic acid capsule is also required by ExPEC strains for virulence in a rat model of meningitis (42), as well as for urothelial cell invasion by K1 UPEC strain UTI89 in a murine UTI model (43). Our finding that capsule contributes to the fitness of UPEC once it gains access to the bloodstream is consistent with these previous reports.

The *nanA* mutant, which lacks the ability to degrade sialic acid, had the largest competitive defect of any mutant tested in our cochallenge model of UPEC bacteremia. Although not required for fitness in the murine urinary tract (9), an *E. coli* MG1655 *nanAT* mutant was defective for the establishment of intestinal colonization in a streptomycin-treated mouse model (44). Thus, it appears that host sialic acid may serve as a preferential carbon source for *E. coli* in the GI tract and bloodstream but not in the urinary tract. Sialic acid also inhibits type 1 fimbriation via repression of the FimB recombinase (45), so it is possible that NanA-mediated sialic acid catabolism is also important for maintaining intracellular sialic acid homeostasis for optimal *fim* expression during UPEC bacteremia.

As for UTI, it appears that the presence of a single virulence factor is not sufficient for the development of UPEC bacteremia. Even *nanA*, which, of the genes tested here, contributed the most to infection, was necessary but not sufficient to allow systemic colonization. *E. coli* strain MG1655 encodes both *nanA* and *fim* but was unable to persist systemically. Although MG1655 also encodes *tonB*, its genome contains fewer TonB-dependent iron acquisition systems; for instance, it lacks a heme uptake system. Consequently, it is probable that the presence of a number of bacteremia fitness determinants allows UPEC survival and systemic dissemination. Other uropathogenicity and nonurovirulence factors likely also contribute to UPEC systemic colonization, and future delineation of these mechanisms in the bacteremia model described here will contribute to our overall understanding of the progression to urosepsis.

MATERIALS AND METHODS

Bacterial strains, plasmids, and culture conditions. The bacterial strains and plasmids used in this study are summarized in Table 2. All strains were cultured in Luria broth (10 g/liter tryptone, 5 g/liter yeast extract, 0.5 g/liter NaCl) or on LB agar with the appropriate antibiotic (100 μg/ml ampicillin, 50 μg/ml nalidixic acid, or 25 μg/ml kanamycin) and incubated at 37°C for 18 h.

Murine model of bacteremia. Female CBA/J mice (The Jackson Laboratory, Bar Harbor, ME) aged 6 to 8 weeks were restrained using a Universal Restrainer (Braintree Scientific, Braintree, MA) and inoculated via the tail vein over a 30-s period with a 100-μl bacterial suspension delivering 10^2 to 10^6 CFU/mouse. The inoculum was prepared by resuspending overnight cultures in phosphate-buffered saline (PBS) and diluting them to 1×10^3 to 1×10^7 CFU/ml. For cochallenges, wild-type and mutant suspensions were mixed 1:1 before inoculation. When appropriate, perfusion was performed on euthanized animals by cutting a small hole in the right cardiac ventricle and infusing the left ventricle slowly with 40 ml 0.9% sterile saline before organ removal. Blanching of the organs occurred with the first 20 ml of sterile saline. Excised tissues were homogenized in 3 ml PBS using a mechanical homogenizer (Omni International, Marietta, GA), and homogenate was plated onto LB agar using an Autoplate 4000 (Spiral Biotech, Norwood, MA) to determine the output number of CFU/g tissue. For cochallenge experiments, homogenate was also plated on appropriate antibiotic-containing agar to differentiate wild-type and mutant strains. CIs were calculated by dividing the ratio of mutant to wild-type bacteria in the output by the ratio of mutant to wild-type

TABLE 2 Bacterial strains and plasmids used in this study

Strain or plasmid	Description[a]	Reference
E. coli		
CFT073	Pyelonephritis isolate	22
CFT073^{Nal}	Spontaneous Nal^r strain of CFT073	35
K-12	MG1655, laboratory strain	47
ksl	UMD141; CFT073 Δ*ksl*(*K2*)*ABCDE*	7
fliC	CFT073 Δ*fliC*::*kan* Kan^r	5
nanA	CFT073 Δ*nanA*::*kan* Kan^r	9
pap	UPEC 76 CFT073 Δ*pap* Δ*pap_2* Nal^r	35
fim L-OFF	CFT073 *fim* phase locked-OFF Nal^r	48
hlyD	CFT073 *hlyD*::Tn*phoA* Kan^r	22
hma chuA	CFT073 Δ*hma*::*kan chuA*::*cat* Kan^r Cam^r	26
tonB	CFT073 Δ*tonB*::*kan* Kan^r	This study
CFT073 *lacZ*	CFT073 Δ*lacZ*::*kan* Kan^r	M. Walters and H. L. T. Mobley, unpublished data
K-12 *lacZ*	K-12 Δ*lacZ*::*kan* Kan^r	This study
Plasmids		
pKD4	λ Red template vector; Kan^r Amp^r	46
pKD46	Red recombinase helper plasmid, temperature sensitive; Amp^r	46
pGEN-*lux*	pGEN-*luxCDABE*, bioluminescent reporter, *em7* promoter; Amp^r	20

[a] Amp, ampicillin; Cam, chloramphenicol; Kan, kanamycin; Nal, nalidixic acid.

bacteria in the input. All animal protocols were approved by the University Committee on Use and Care of Animals at the University of Michigan Medical School. Statistical significance was determined using GraphPad Prism 5 for independent challenges using the Mann-Whitney test and for cochallenges using the Wilcoxon signed-rank test (with a hypothetical value of 0) on log-transformed CI values.

***In vivo* bioluminescent imaging.** Imaging was performed as described previously (20). The hair was completely removed from the dorsal and ventral sides of anesthetized mice using a Cordless Rechargeable Animal Trimmer Series 8900 (Wahl, United States) and cosmetic hair removal treatment (Sensitive Skin VEET; Reckitt Benckiser, Parsippany, NJ). Mice were inoculated as described above with *E. coli* CFT073(pGEN-*lux*) and imaged at various time points using an IVIS 200 imaging system (Xenogen) with a 5-min exposure time. During imaging, mice were anesthetized in chambers containing 2.0% isoflurane inhalant mixed with oxygen (Baxter, Deerfield, IL) via an IVIS manifold placed within the imaging chamber. Photon emissions were obtained using the Living Image software (Xenogen).

Mutant construction. Isogenic *E. coli* CFT073 *tonB* and *E. coli* MG1644 *lacZ* mutants (Table 2) were constructed using the λ Red recombinase system (46). A kanamycin resistance cassette was PCR amplified from pKD4 (Table 2) using primers containing sequences in the 5′ and 3′ ends of *tonB* or *lacZ*. This product was used to replace >80% of the *tonB* or *lacZ* gene by Red recombinase-mediated homologous recombination (recombinase expressed from pKD46) in CFT073 or MG1655. Mutants were verified by PCR, differential EagI digestion, and for the *lacZ* mutant, verification of a white-colony phenotype on 80 μg/ml 5-bromo-4-chloro-3-indolyl-β-D-galactopyranoside (X-Gal) agar.

ACKNOWLEDGMENTS

We thank Michael Donnenberg (University of Maryland School of Medicine) for generously providing the UMD141 (CFT073 Δ*ksl*) strain, the University of Michigan Center for Molecular Imaging, Kathryn Eaton for technical advice, Christopher Alteri for the CFT073 Δ*nanA* strain, and Matthew Walters for the CFT073 Δ*lacZ* strain.

This work was supported by Public Health Service grants AI43363 and AI059722 from the National Institutes of Health.

REFERENCES

1. **Al-Hasan, M. N., J. E. Eckel-Passow, and L. M. Baddour.** 2010. Bacteremia complicating gram-negative urinary tract infections: a population-based study. J. Infect. **60**:278–285.
2. **Johnson, D. E., R. G. Russell, C. V. Lockatell, J. C. Zulty, and J. W. Warren.** 1993. Urethral obstruction of 6 hours or less causes bacteriuria, bacteremia, and pyelonephritis in mice challenged with "nonuropathogenic" *Escherichia coli*. Infect. Immun. **61**:3422–3428.
3. **Connell, I., W. Agace, P. Klemm, M. Schembri, S. Marild, and C. Svanborg.** 1996. Type 1 fimbrial expression enhances *Escherichia coli* virulence for the urinary tract. Proc. Natl. Acad. Sci. U. S. A. **93**:9827–9832.
4. **Goluszko, P., S. L. Moseley, L. D. Truong, A. Kaul, J. R. Williford, R. Selvarangan, S. Nowicki, and B. Nowicki.** 1997. Development of experimental model of chronic pyelonephritis with *Escherichia coli* O75:K5:H-bearing Dr fimbriae: mutation in the dra region prevented tubulointerstitial nephritis. J. Clin. Invest. **99**:1662–1672.
5. **Lane, M. C., V. Lockatell, G. Monterosso, D. Lamphier, J. Weinert, J. R. Hebel, D. E. Johnson, and H. L. Mobley.** 2005. Role of motility in the colonization of uropathogenic *Escherichia coli* in the urinary tract. Infect. Immun. **73**:7644–7656.
6. **Rippere-Lampe, K. E., A. D. O'Brien, R. Conran, and H. A. Lockman.** 2001. Mutation of the gene encoding cytotoxic necrotizing factor type 1 (cnf_1) attenuates the virulence of uropathogenic *Escherichia coli*. Infect. Immun. **69**:3954–3964.
7. **Buckles, E. L., X. Wang, M. C. Lane, C. V. Lockatell, D. E. Johnson, D. A. Rasko, H. L. Mobley, and M. S. Donnenberg.** 2009. Role of the K2 capsule in *Escherichia coli* urinary tract infection and serum resistance. J. Infect. Dis. **199**:1689–1697.
8. **Torres, A. G., P. Redford, R. A. Welch, and S. M. Payne.** 2001. TonB-dependent systems of uropathogenic *Escherichia coli*: aerobactin and heme transport and TonB are required for virulence in the mouse. Infect. Immun. **69**:6179–6185.
9. **Alteri, C. J., S. N. Smith, and H. L. Mobley.** 2009. Fitness of *Escherichia coli* during urinary tract infection requires gluconeogenesis and the TCA cycle. PLoS Pathog. **5**:e1000448.
10. **Russo, T. A., S. T. Jodush, J. J. Brown, and J. R. Johnson.** 1996. Identification of two previously unrecognized genes (*guaA* and *argC*) important for uropathogenesis. Mol. Microbiol. **22**:217–229.
11. **Brzuszkiewicz, E., H. Bruggemann, H. Liesegang, M. Emmerth, T. Olschlager, G. Nagy, K. Albermann, C. Wagner, C. Buchrieser, L. Emody, G. Gottschalk, J. Hacker, and U. Dobrindt.** 2006. How to become a uropathogen: comparative genomic analysis of extraintestinal pathogenic *Escherichia coli* strains. Proc. Natl. Acad. Sci. U. S. A. **103**:12879–12884.
12. **Blanco, M., J. E. Blanco, M. P. Alonso, and J. Blanco.** 1994. Virulence factors and O groups of *Escherichia coli* strains isolated from cultures of blood specimens from urosepsis and non-urosepsis patients. Microbiologia **10**:249–256.
13. **Johnson, J. R., S. L. Moseley, P. L. Roberts, and W. E. Stamm.** 1988. Aerobactin and other virulence factor genes among strains of *Escherichia coli* causing urosepsis: association with patient characteristics. Infect. Immun. **56**:405–412.

14. **Johnson, J. R., and A. L. Stell.** 2000. Extended virulence genotypes of *Escherichia coli* strains from patients with urosepsis in relation to phylogeny and host compromise. J. Infect. Dis. **181**:261–272.
15. **Picard, B., J. S. Garcia, S. Gouriou, P. Duriez, N. Brahimi, E. Bingen, J. Elion, and E. Denamur.** 1999. The link between phylogeny and virulence in *Escherichia coli* extraintestinal infection. Infect. Immun. **67**:546–553.
16. **Schubert, S., B. Picard, S. Gouriou, J. Heesemann, and E. Denamur.** 2002. Yersinia high-pathogenicity island contributes to virulence in *Escherichia coli* causing extraintestinal infections. Infect. Immun. **70**: 5335–5337.
17. **Durant, L., A. Metais, C. Soulama-Mouze, J. M. Genevard, X. Nassif, and S. Escaich.** 2007. Identification of candidates for a subunit vaccine against extraintestinal pathogenic *Escherichia coli*. Infect. Immun. **75**: 1916–1925.
18. **Diard, M., S. Baeriswyl, O. Clermont, S. Gouriou, B. Picard, F. Taddei, E. Denamur, and I. Matic.** 2007. *Caenorhabditis elegans* as a simple model to study phenotypic and genetic virulence determinants of extraintestinal pathogenic *Escherichia coli*. Microbes Infect. **9**:214–223.
19. **Khan, N. A., and G. J. Goldsworthy.** 2007. Novel model to study virulence determinants of *Escherichia coli* K1. Infect. Immun. **75**:5735–5739.
20. **Lane, M. C., C. J. Alteri, S. N. Smith, and H. L. Mobley.** 2007. Expression of flagella is coincident with uropathogenic *Escherichia coli* ascension to the upper urinary tract. Proc. Natl. Acad. Sci. U. S. A. **104**: 16669–16674.
21. **Wiles, T. J., J. M. Bower, M. J. Redd, and M. A. Mulvey.** 2009. Use of zebrafish to probe the divergent virulence potentials and toxin requirements of extraintestinal pathogenic *Escherichia coli*. PLoS Pathog. **5**:e1000697.
22. **Mobley, H. L., D. M. Green, A. L. Trifillis, D. E. Johnson, G. R. Chippendale, C. V. Lockatell, B. D. Jones, and J. W. Warren.** 1990. Pyelonephritogenic *Escherichia coli* and killing of cultured human renal proximal tubular epithelial cells: role of hemolysin in some strains. Infect. Immun. **58**:1281–1289.
23. **Hopkins, W. J., J. A. Hall, B. P. Conway, and D. T. Uehling.** 1995. Induction of urinary tract infection by intraurethral inoculation with *Escherichia coli*: refining the murine model. J. Infect. Dis. **171**:462–465.
24. **Zhou, Y. Q., L. Davidson, R. M. Henkelman, B. J. Nieman, F. S. Foster, L. X. Yu, and X. J. Chen.** 2004. Ultrasound-guided left-ventricular catheterization: a novel method of whole mouse perfusion for microimaging. Lab. Invest. **84**:385–389.
25. **Smith, Y. C., S. B. Rasmussen, K. K. Grande, R. M. Conran, and A. D. O'Brien.** 2008. Hemolysin of uropathogenic *Escherichia coli* evokes extensive shedding of the uroepithelium and hemorrhage in bladder tissue within the first 24 hours after intraurethral inoculation of mice. Infect. Immun. **76**:2978–2990.
26. **Hagan, E. C., and H. L. Mobley.** 2009. Haem acquisition is facilitated by a novel receptor Hma and required by uropathogenic *Escherichia coli* for kidney infection. Mol. Microbiol. **7**:79–91.
27. **Vimr, E. R., and F. A. Troy.** 1985. Regulation of sialic acid metabolism in *Escherichia coli*: role of *N*-acylneuraminate pyruvate-lyase. J. Bacteriol. **164**:854–860.
28. **Hopkins, W. J., A. Gendron-Fitzpatrick, E. Balish, and D. T. Uehling.** 1998. Time course and host responses to *Escherichia coli* urinary tract infection in genetically distinct mouse strains. Infect. Immun. **66**: 2798–2802.
29. **Bortolussi, R., P. Ferrieri, and L. W. Wannamaker.** 1978. Dynamics of *Escherichia coli* infection and meningitis in infant rats. Infect. Immun. **22**:480–485.
30. **Robbins, J. B., G. H. McCracken, Jr., E. C. Gotschlich, F. Orskov, I. Orskov, and L. A. Hanson.** 1974. *Escherichia coli* K1 capsular polysaccharide associated with neonatal meningitis. N. Engl. J. Med. **290**:1216–1220.
31. **Huang, S. H., C. Wass, Q. Fu, N. V. Prasadarao, M. Stins, and K. S. Kim.** 1995. *Escherichia coli* invasion of brain microvascular endothelial cells in vitro and in vivo: molecular cloning and characterization of invasion gene *ibe10*. Infect. Immun. **63**:4470–4475.
32. **Hoffman, J. A., C. Wass, M. F. Stins, and K. S. Kim.** 1999. The capsule supports survival but not traversal of *Escherichia coli* K1 across the blood-brain barrier. Infect. Immun. **67**:3566–3570.
33. **Teng, C. H., M. Cai, S. Shin, Y. Xie, K. J. Kim, N. A. Khan, F. Di Cello, and K. S. Kim.** 2005. *Escherichia coli* K1 RS218 interacts with human brain microvascular endothelial cells via type 1 fimbria bacteria in the fimbriated state. Infect. Immun. **73**:2923–2931.
34. **Xie, Y., Y. Yao, V. Kolisnychenko, C. H. Teng, and K. S. Kim.** 2006. HbiF regulates type 1 fimbriation independently of FimB and FimE. Infect. Immun. **74**:4039–4047.
35. **Mobley, H. L., K. G. Jarvis, J. P. Elwood, D. I. Whittle, C. V. Lockatell, R. G. Russell, D. E. Johnson, M. S. Donnenberg, and J. W. Warren.** 1993. Isogenic P-fimbrial deletion mutants of pyelonephritogenic *Escherichia coli*: the role of alpha Gal(1-4) beta Gal binding in virulence of a wild-type strain. Mol. Microbiol. **10**:143–155.
36. **Kallenius, G., S. Svenson, R. Mollby, B. Cedergren, H. Hultberg, and J. Winberg.** 1981. Structure of carbohydrate part of receptor on human uroepithelial cells for pyelonephritogenic *Escherichia coli*. Lancet **ii**: 604–606.
37. **Kallenius, G., R. Mollby, S. B. Svenson, J. Winberg, and H. Hultberg.** 1980. Identification of a carbohydrate receptor recognized by uropathogenic *Escherichia coli*. Infection **8**(Suppl. 3):288–293.
38. **Xie, Y., V. Kolisnychenko, M. Paul-Satyaseela, S. Elliott, G. Parthasarathy, Y. Yao, G. Plunkett III, F. R. Blattner, and K. S. Kim.** 2006. Identification and characterization of *Escherichia coli* RS218-derived islands in the pathogenesis of *E. coli* meningitis. J. Infect. Dis. **194**:358–364.
39. **Torres, A. G., and S. M. Payne.** 1997. Haem iron-transport system in enterohaemorrhagic *Escherichia coli* O157:H7. Mol. Microbiol. **23**: 825–833.
40. **Leveille, S., M. Caza, J. R. Johnson, C. Clabots, M. Sabri, and C. M. Dozois.** 2006. Iha from an *Escherichia coli* urinary tract infection outbreak clonal group A strain is expressed in vivo in the mouse urinary tract and functions as a catecholate siderophore receptor. Infect. Immun. **74**: 3427–3436.
41. **Zhao, L., S. Gao, H. Huan, X. Xu, X. Zhu, W. Yang, Q. Gao, and X. Liu.** 2009. Comparison of virulence factors and expression of specific genes between uropathogenic *Escherichia coli* and avian pathogenic *E. coli* in a murine urinary tract infection model and a chicken challenge model. Microbiology **155**:1634–1644.
42. **Kim, K. S., H. Itabashi, P. Gemski, J. Sadoff, R. L. Warren, and A. S. Cross.** 1992. The K1 capsule is the critical determinant in the development of *Escherichia coli* meningitis in the rat. J. Clin. Invest. **90**:897–905.
43. **Anderson, G. G., C. C. Goller, S. Justice, S. J. Hultgren, and P. C. Seed.** 2010. Polysaccharide capsule and sialic acid-mediated regulation promote biofilm-like intracellular bacterial communities during cystitis. Infect. Immun. **78**:963–975.
44. **Chang, D. E., D. J. Smalley, D. L. Tucker, M. P. Leatham, W. E. Norris, S. J. Stevenson, A. B. Anderson, J. E. Grissom, D. C. Laux, P. S. Cohen, and T. Conway.** 2004. Carbon nutrition of *Escherichia coli* in the mouse intestine. Proc. Natl. Acad. Sci. U. S. A. **101**:7427–7432.
45. **El-Labany, S., B. K. Sohanpal, M. Lahooti, R. Akerman, and I. C. Blomfield.** 2003. Distant cis-active sequences and sialic acid control the expression of *fimB* in *Escherichia coli* K-12. Mol. Microbiol. **49**:1109–1118.
46. **Datsenko, K. A., and B. L. Wanner.** 2000. One-step inactivation of chromosomal genes in *Escherichia coli* K-12 using PCR products. Proc. Natl. Acad. Sci. U. S. A. **97**:6640–6645.
47. **Blattner, F. R., G. Plunkett III, C. A. Bloch, N. T. Perna, V. Burland, M. Riley, J. Collado-Vides, J. D. Glasner, C. K. Rode, G. F. Mayhew, J. Gregor, N. W. Davis, H. A. Kirkpatrick, M. A. Goeden, D. J. Rose, B. Mau, and Y. Shao.** 1997. The complete genome sequence of *Escherichia coli* K-12. Science **277**:1453–1462.
48. **Gunther, N. W., J. A. Snyder, V. Lockatell, I. Blomfield, D. E. Johnson, and H. L. T. Mobley.** 2002. Assessment of virulence of uropathogenic *Escherichia coli* type 1 fimbrial mutants in which the invertible element is phase-locked on or off. Infect. Immun. **70**:3344–3354.